JOURNAL OF SPACECRAFT AND ROCKETS
Vol. 40, No. 1, January–February 2003

Semiempirical Method for Predicting Aerodynamics of Trailing-Edge Flaps

F. G. Moore*
Aeroprediction, Inc., King George, Virginia 22485
and
T. C. Hymer†
U.S. Naval Surface Warfare Center, Dahlgren, Virginia 22448

An improved semiempirical method has been developed to estimate the static aerodynamics of configurations that use a trailing-edge flap for control. The method is based on deflecting the full aft-located lifting surface by an amount that allows the normal force coefficient to be equal to that generated by the deflected flap. A transfer in pitching moments and a modified axial force coefficient is derived to complete the set of static aerodynamics. The method is derived using theoretical methods that are a part of the 1998 version of the U.S. Naval Surface Warfare Center aeroprediction code and two sets of experimental data. Comparison of the improved method to available data shows that the method gives satisfactory results over the practical range for which trailing-edge flaps are contemplated for use. This practical range is an angle of attack less than 10 deg, Mach number of 2.0 or less, and flap deflections of less than 30 deg. However, additional wind-tunnel data are needed to refine and expand the applicability of the method. The additional wind-tunnel data requirement is particularly true for transonic Mach numbers and for supersonic Mach numbers where the angle of attack and control deflection are of the same sign.

Nomenclature

AR	=	aspect ratio, b^2/A_W
A_{ref}	=	reference area (maximum cross-sectional area of body, if a body is present, or planform area of wing, if wing alone), ft^2
A_W	=	planform area of wing in crossflow plane, ft^2
b	=	wing span (not including body), ft
C_A	=	axial force coefficient
C_M	=	pitching moment coefficient (based on reference area and body diameter, if body present, or mean aerodynamic chord, if wing alone)
C_N	=	normal force coefficient
$C_{N_{B(W)}}$, $C_{N_{B(T)}}$	=	normal force coefficient on body in presence of wing or tail
C_{N_W}	=	normal force coefficient of wing alone
$C_{N_{W(B)}}$, $C_{N_{T(B)}}$	=	normal force coefficient of wing or tail in presence of body
C_{N_α}	=	normal force coefficient derivative
$(C_{N_\alpha})_W$, $(C_{N_\alpha})_T$	=	normal force coefficient slope of wing and tail, respectively
c_r	=	root chord, ft
c_{r_w}, c_{r_f}	=	root chord of wing and flap, respectively, ft
c_t	=	tip chord, ft
d_B	=	body diameter, at base, ft
d_{ref}	=	reference body diameter, ft
f_1, f_2, f_3	=	empirical factors used in defining the semiempirical model for flap aerodynamics
$k_{B(W)}$, $k_{B(T)}$	=	ratio of additional body normal-force coefficient due to presence of wing or tail at a control deflection to that of wing or tail alone at $\alpha = 0$ deg
$k_{W(B)}$, $k_{T(B)}$	=	ratio of wing or tail normal force coefficient in presence of body due to a control deflection to that of wing or tail alone at $\alpha = 0$ deg
ℓ, ℓ_n	=	total length and nose length, respectively, ft
ℓ_{ref}	=	reference length, ft
$M_{W(B)}$, $M_{B(W)}$	=	moment of wing in presence of body and body in presence of wing, respectively, ft · lb
M_∞	=	freestream Mach number
N_f	=	normal force of trailing-edge flap, lb
$N_{W(B)}$, $N_{B(W)}$	=	normal force of wing in presence of body and body in presence of wing, respectively, lb
R_N	=	Reynolds number
r_{LE}, r_{TE}	=	radius of leading and trailing edges of fin, respectively, ft
r_n	=	nose radius, ft
t	=	fin thickness, ft
X_{LE}, X_{CG}	=	distance from nose tip to wing leading edge or c.g. of body, respectively, ft
X_{CP}	=	c.p. in x direction, in feet or calibers from some reference point that can be specified
X_{ref}	=	reference location along x axis for moments, ft
x, y, z	=	axis system fixed with x along centerline of body
α	=	angle of attack, deg
α_{TR}	=	trim angle of attack, deg
$(\Delta C_A)_f$, $(\Delta C_N)_f$, $(\Delta C_M)_f$	=	change in axial, normal, and pitching moment coefficients, respectively, due to a flap deflection δ_f
δ_f	=	control deflection of trailing-edge flap, positive leading edge up, deg
δ_W, δ_T	=	deflection of wing or tail surfaces, positive leading edge up, deg
Λ_{LE}	=	leading-edge sweepback angle of fin, deg
λ	=	taper ratio of a lifting surface, c_t/c_r

Received 10 December 2001; revision received 2 September 2002; accepted for publication 20 September 2002.

*President, 9449 Grover Drive, Suite 201. Associate Fellow AIAA.
†Aerospace Engineer, Missile Systems Engineering Branch, Weapons Systems Department, Dahlgren Division. Member AIAA.

Φ = roll position of missile fins [$\Phi = 0$ deg corresponds to fins in the plus (+) orientation, and $\Phi = 45$ deg corresponds to fins rolled to the cross (×) orientation]

Introduction

ONE idea that has been considered to meet lower-cost, lower-volume, and lower-maneuverability control requirements of guided projectiles is to deflect a part of a wing or tail surface as opposed to the entire surface. The portion of the tail surface considered for deflection is at the tail or wing trailing edge. Figure 1 is a typical concept being considered, where a part of the trailing-edge portion of the tail fin is being considered for the control surface as opposed to the entire tail surface. As seen in Fig. 1, this projectile concept is very low drag and, given a high initial velocity, can produce a fairly long range, even without a rocket motor. Long ranges, winds, and other ballistic errors can produce sizable miss distances without some sort of corrective device. Whereas the large tail fins of the Fig. 1 concept are needed for stability at a high-velocity launch, deflecting the entire tail fin by a significant amount to eliminate the ballistic errors is not necessary. Only a fraction of the tail surface is required to provide adequate maneuverability if the deflection occurs over a sustained period of time. The small deflected surface area can also result in a much lower volume, weight, and cost for the control system. As seen in Fig. 1, the amount of area of the trailing edge can vary depending on the requirements. Shown in Fig. 1 is a variable semispan, root chord, and hinge line for the trailing-edge flap.

The most recent version of the U.S. Naval Surface Warfare Center aeroprediction code AP98[1] distributed to users is not capable of computing aerodynamics on a concept such as that shown in Fig. 1 when the trailing-edge flaps are deflected. The objective of this paper is to develop the methodology to allow the 2002 version of the aeroprediction code (AP02) to compute aerodynamics on a configuration where some portion of the rear part of the aft lifting surface (either wing or tail) can be deflected to provide control. In developing this trailing-edge flap aerodynamic predictive methodology, considerations of the cost to integrate the new methodology into the aeroprediction code (APC) was a prime driver in the method chosen. The APC is currently set up configurationwise to handle wing–body–tail configurations with control deflections allowed on the full wing or full tail. Hence, from a cost standpoint, it is desirable to develop a methodology that fits into this logic. The work discussed in this paper is described in more detail in Ref. 2.

In reviewing the literature to determine approaches to use for calculating the aerodynamics of trailing-edge flaps, the general approach that comes closest to that desired for use in the future AP02 is that adopted for the Missile Datcom.[3] In that approach, an equivalent value of deflection for the entire wing or tail surface is determined to reflect a given flap deflection. In other words,

$$\delta_W = f(\delta_f) \tag{1}$$

The equivalent value of δ_W is determined offline using methods in the airplane DATCOM[4] at subsonic speeds and the method of Goin[5] at supersonic speeds. The advantage of an approach such as Eq. (1) for codes such as Missile Datcom[3] or AP98[1] is that this is the least costly and most straightforward approach to incorporating the computation of aerodynamics of trailing-edge flaps into an existing computer code. The low cost is because codes such as AP98[1] or Missile Datcom[3] are generally already set up logicwise to compute the aerodynamics of a configuration where one set of fins are deflected. Hence, if one can define what that wing deflection is in terms of some flap deflection, the codes[1,3] can be exercised to provide a set of aerodynamics that simulate a configuration with a trailing-edge flap deflected by a given amount.

Although the approach used by the Missile Datcom [Eq. (1)] to compute aerodynamics of trailing-edge flaps is the same approach that will be adopted for use here, the methods that will be used for the AP02 will differ from those[4,5] used in the Missile Datcom.[3] There are several reasons for this. First, the method of Goin[5] has too many limitations. Some of these limitations include requirements for supersonic leading and trailing edges of the flap hinge line, viscous effects are not accounted for, and the method does not include nonlinearities due to large flap deflections or angles of attack (AOA). Second, whereas the method of Ref. 4 takes into account some of the viscous and nonlinear effects that Ref. 5 does not account for, the method itself is inconsistent with that of Ref. 5.

The objective here is, thus, to derive an improved method to compute aerodynamics of trailing-edge flaps that utilize the Eq. (1) approach. The method should be similar for both subsonic and supersonic freestream Mach numbers, should not be limited to supersonic

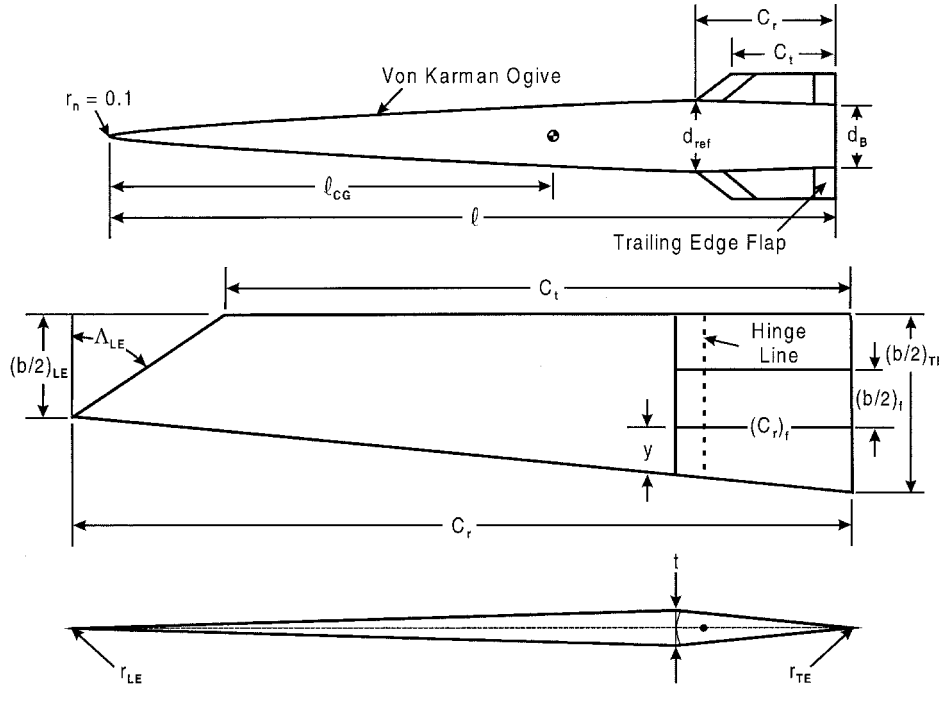

Fig. 1 Projectile concept where tail trailing-edge flap is deflected for control.

leading and trailing edges, should account (at least empirically) for viscous effects, and should account for nonlinearities associated with large flap deflections or AOA. From a practical standpoint, the weapons that will use the trailing-edge flaps for control will typically fly at fairly small trim AOA (less than 10 deg). However, flap deflections as large as ±30 deg are not unreasonable to achieve the appropriate trim AOA desired. Also, from a practical standpoint, most applications the authors are aware of will be below $M_\infty = 2.0$. However, the method should be general enough to be applied over the Mach number range of applicability of the AP98 or AP02, which is from 0 to 20. On the other hand, the method will not be validated over this large Mach number range due to limited experimental data and Navier–Stokes computations.

Analysis

To implement the methodology for computing the aerodynamics of a weapon concept that is controlled by trailing-edge flaps most efficiently, we will seek the definition of the equivalent wing deflection that yields the same normal force, pitching moment, and trim AOA as that obtained by deflecting the trailing-edge flaps. In mathematical terms,

$$N_{W(B)} + N_{B(W)} = N_f f_1 \tag{2}$$

$$M_{W(B)} + M_{B(W)} = N_f f_1[(X_{\mathrm{CP}})_f - X_{\mathrm{ref}}] \tag{3}$$

$$(\alpha_{\mathrm{TR}})_W = (\alpha_{\mathrm{TR}})_f \tag{4}$$

In reality, if Eqs. (2) and (3) are satisfied, Eq. (4) will automatically be satisfied. We, thus, must define the relationships that allow Eqs. (2) and (3) to be satisfied.

Notice that, in Eqs. (2) and (3), the wing–body normal force and pitching moments are equated to the normal force and pitching moment coefficients of the flap alone, with no interference effects present, multiplied by an empirical constant. There are a couple of reasons for this. First, when the entire wing is deflected it will have carryover normal force onto the wing. This carryover normal force means the equivalent control deflection of the entire wing will be lower than if no carryover normal force were present. Second, whereas there will be some interference carryover normal force onto the flap from the wing or body, this extra normal force can be lumped into an empirical term f_1, which will be defined later.

Equation (2) can be expanded as

$$\left(C_{N_\alpha}\right)_W \left[k_{W(B)} + k_{B(W)}\right]\delta_W = \left(C_{N_\alpha}\right)_f f_1 \delta_f \tag{5}$$

The empirical factor f_1 in Eq. (5) accounts for several physical phenomena. These physical phenomena include boundary-layer buildup and separation of the flow ahead of the flap on the wing surface, flap thickness effects, effects of the slot created between the wing and flap when the flap is deflected, and interference effects of the flap onto the body or wing, or the wing or body onto the flap. The factor f_1 will be determined empirically based on experimental data for wings that have trailing-edge flaps. Figure 2 attempts to show pictorially and mathematically the representation of a trailing-edge flap deflection by deflecting the full wing.

To determine f_1, we equate the right-hand side of Eq. (5) to the change in normal force coefficient at some AOA due to a control deflection δ_f. That is,

$$f_1 = \frac{(\Delta C_N)_f}{\left(C_{N_\alpha}\right)_f \delta_f f_2} \tag{6}$$

$(\Delta C_N)_f$ of Eq. (6) is the additional normal force coefficient created by a flap deflection δ_f. $(C_{N_\alpha})_f$ is the theoretical normal force coefficient slope for the flap of given aspect ratio and taper ratio at a given Mach number and AOA. This theoretical value is determined by the methods in the AP02 for a flap only (no wing ahead of it). The AP02 methods include linearized theories at low AOA or control deflection combined with empirical approaches at higher AOA. These methods in the AP98 or AP02 are fairly general and can calculate aerodynamics on supersonic or subsonic leading-edge wings or flaps at low AOA. Also, aerodynamics can be computed for Mach numbers 0–20 and AOA to 90 deg. Hence, the theoretical methodology for computing $(C_{N_\alpha})_f$ is fairly general. The value of $(C_{N_\alpha})_f$ is actually computed using a secant slope for a given AOA. This value of $(C_{N_\alpha})_f$ is then multiplied by the given flap deflection δ_f, as seen in Eq. (6). The numerator of Eq. (6) is based on experimental data, which account for various physical phenomena of a flap in

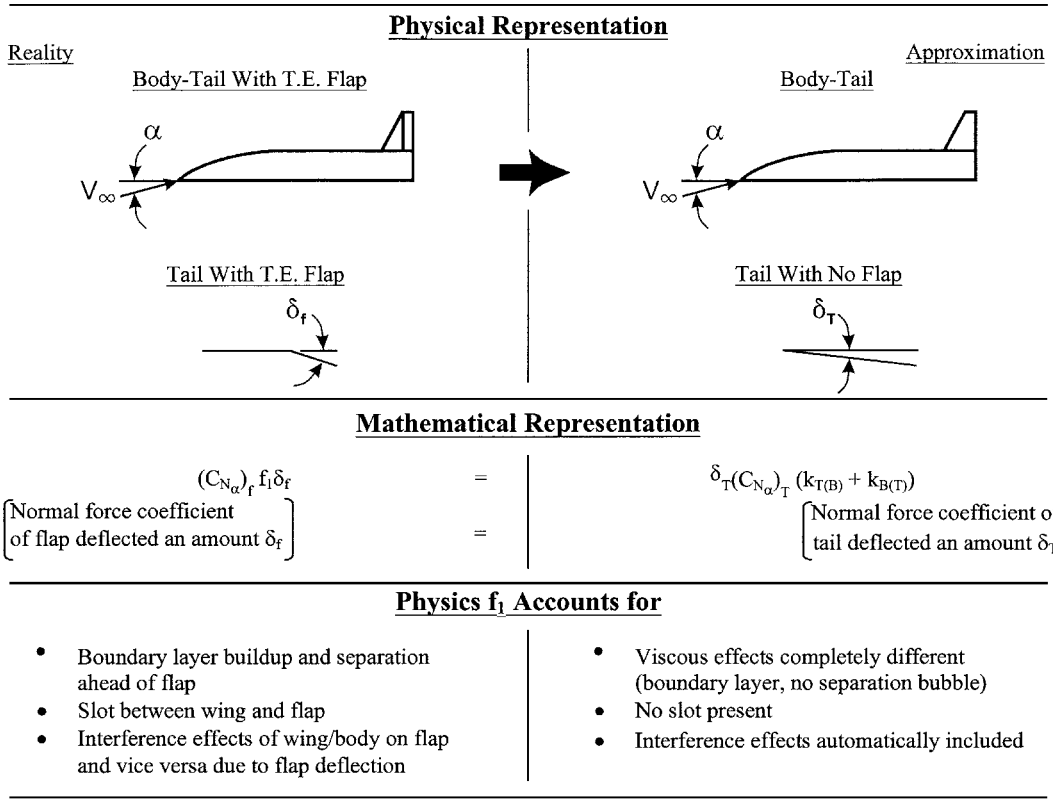

Fig. 2 Physical and mathematical representation of trailing-edge flap deflection by full wing deflection.

conjunction with a wing, which a wing alone does not have. Hence, the empirical factor f_1 is generated by the ratio of experimental data for a flap on a wing to a theoretical wing-alone solution.

The factor f_2 in the denominator of Eq. (6) is used to account for the fact that the theory in the AP02 that defines the lift curve slope of an entire wing deflected an by amount δ at a given AOA may not accurately predict the increment in normal force generated by a flap. The factor f_2 is expected to be near one at supersonic speeds. However, at subsonic speeds, wind-tunnel data suggest that the theoretical predictions of additional normal force generated by a flap are higher than what the theory suggests. This inaccuracy of the theory arises from using the secant slope for $(C_{N_\alpha})_f$ vs using the local slope at a given value of α. At supersonic speeds, use of the secant slope does not appear to be a problem. However, subsonically, the C_N vs α curve levels out at around 25–30 deg AOA, and so an additional increase in α brings increasingly less increase in C_N. Using a secant slope for $(C_{N_\alpha})_f$ vs the local tangent gives a value of $(C_{N_\alpha})_f$ that is too large and, therefore, a value of f_1 that is too low. The parameter f_2, therefore, corrects for this weakness. One could change the overall AP02 code to use local vs secant slopes. However, this would be a very costly and time-consuming process, and it was much more cost effective to define the factor f_2 to take care of this correction for the trailing-edge flap technology.

In Eq. (6), it is assumed that both the numerator and denominator are based on the same reference area A_{ref}. If $(C_{N_\alpha})_f$ is calculated based on a wing-alone solution for the flap, then Eq. (6) must be multiplied by A_{ref}/A_f to have consistent reference areas.

To define the empirical factor f_1, two databases will be used.[6,7] Reference 6 contains data for a canard–body–tail configuration (Fig. 3) with trailing-edge flaps. Data are available for Mach numbers 1.5–4.63, AOA from -2 to about 30 deg (except for $M_\infty = 1.5$, where some data are available only to about 15-deg AOA), and control deflections of 0–30 deg. Unfortunately, no positive values of δ_f were available in Ref. 6, probably because a negative value of δ_f is required for trim to occur when α is positive.

Reference 7 contains data for low Mach numbers ($M_\infty = 0.3$–0.5) for several different configurations. These configurations included an elliptical and a circular cylinder-shaped body with either a delta or sweptback rectangular wing. The wings could have either a leading- or trailing-edge flap. The configuration of most interest here is the delta wing with trailing-edge flaps on a circular cylinder body (Fig. 4). Data are available to 40-deg AOA for flap deflections of ± 10 and ± 30 deg. Hence, Ref. 7 will complement the supersonic data of Ref. 6.

For Mach numbers between $M_\infty = 0.4$ and 1.5, the following procedure will apply for computing f_1. For Mach numbers below $M_\infty = 0.8$, the value of f_1 computed at $M_\infty = 0.4$ will be assumed to apply. For Mach numbers between $M_\infty = 1.5$ and 0.8, linear interpolation will be used to compute f_1 based on the values of f_1 at $M_\infty = 1.5$ and 0.8.

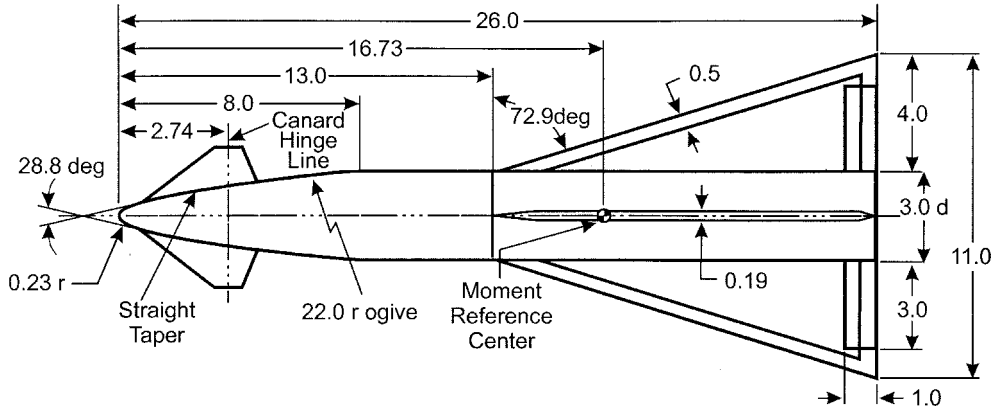

Fig. 3 Model used for supersonic tests[6] (all linear dimensions in inches).

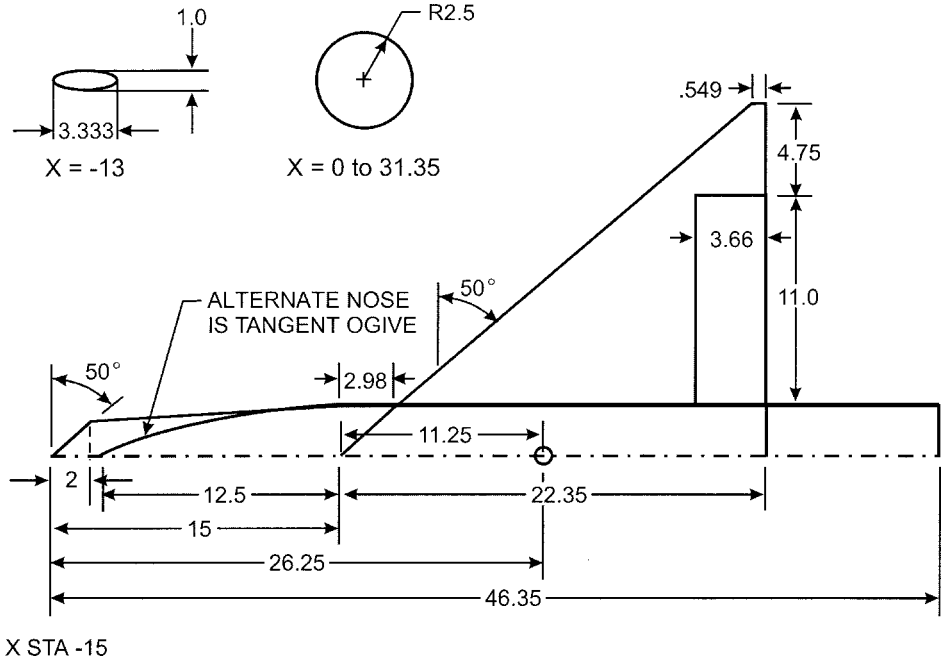

Fig. 4 Delta wing planform used for subsonic tests[7] (all dimensions in inches).

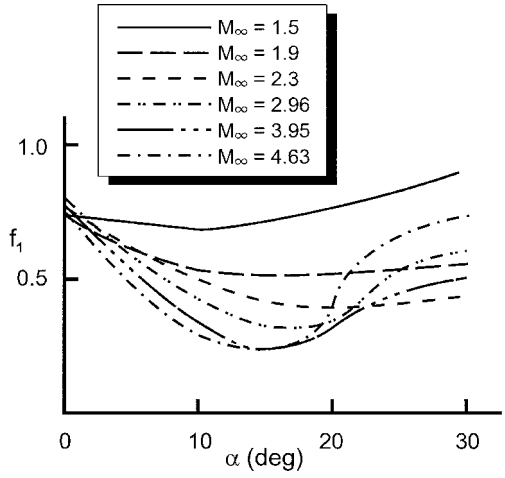

Fig. 5 Value of parameter f_1 at supersonic speeds based on Ref. 6 data and AP98.

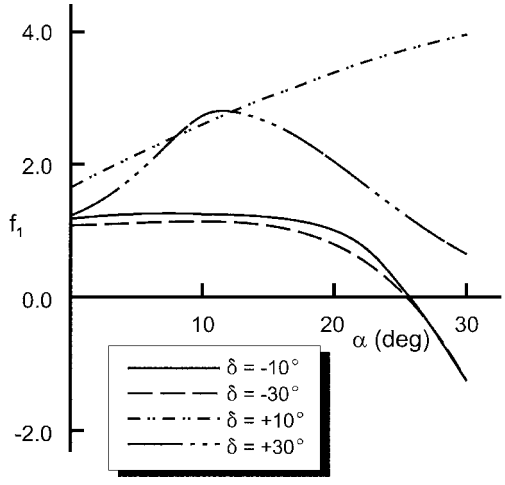

Fig. 6 Value of parameter f_1 at subsonic speeds based on Ref. 7 data and AP98.

Figures 5 and 6 give the values of f_1 determined by using Refs. 6 and 7 to find values of $(\Delta C_N)_f$ and Ref. 1 to compute a value of $(C_{N_\alpha})_f$ at a given AOA. Figure 5 was derived for α and δ of opposite signs, which is the practical case for trim when the aft-located control surface is deflected. Figure 5 also applies for $M_\infty \geq 1.5$ and for values of α and δ of the same sign when α is numerically small. No data have been found to ascertain the validity of Fig. 5 when α and δ are the same sign and α is greater than a small value. For $M_\infty > 4.63$, the value of f_1 at $M_\infty = 4.63$ will be assumed. Also, Fig. 5 holds for values of δ_f up to -30 deg, based on the Ref. 6 data.

Figure 6 gives values of f_1 for $M_\infty = 0.4$ for values of α up to 30 deg and for values of δ_f of ± 30 deg. Figure 6 values of f_1 utilize the values of f_2 from Fig. 7. Figure 7a presents the most practical case for tail-located trailing-edge flaps because α and δ_f must be of opposite signs for trim to occur. Figures 7b and 7c present results for f_2 when α and δ_f are of the same sign. Figure 7b is for $\delta_f = 10$ deg and Fig. 7c is for $\delta_f = 30$ deg. Linear interpolation of Figs. 7b and 7c will occur for values of δ_f other than 10 or 30 deg.

Given f_1 from Figs. 5 or 6, Eq. (5) can be rewritten as

$$\delta_W = \left[\frac{\left(C_{N_\alpha}\right)_f f_1}{\left(C_{N_\alpha}\right)_W \left(k_{W(B)} + k_{B(W)}\right)} \right] \delta_f \qquad (7)$$

The way in which Eq. (7) is utilized within the AP02 is as follows. First, for a given flap size, $(C_{N_\alpha})_f$ is computed from the wing-alone solution in the AP02 at a given M_∞, α, AR, and λ. This value of $(C_{N_\alpha})_f$ is then related to A_{ref} vs A_f. Second, f_1 is then computed via table lookup for a given value of α and M_∞ if the flow is supersonic and for a given value of α, M_∞, and δ_f if the flow is subsonic.

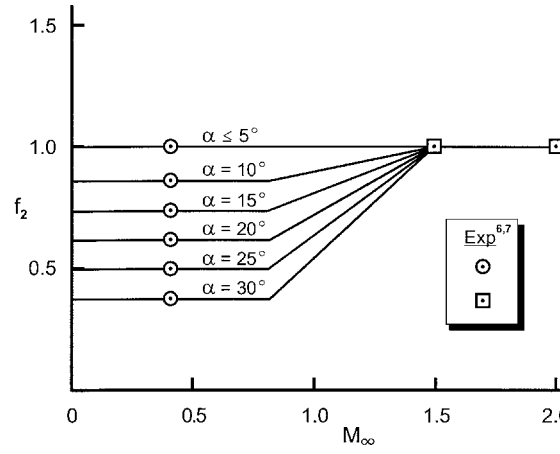

Fig. 7a Factor that corrects for use of secant vs tangent in normal force curve slope (α and δ of opposite signs).

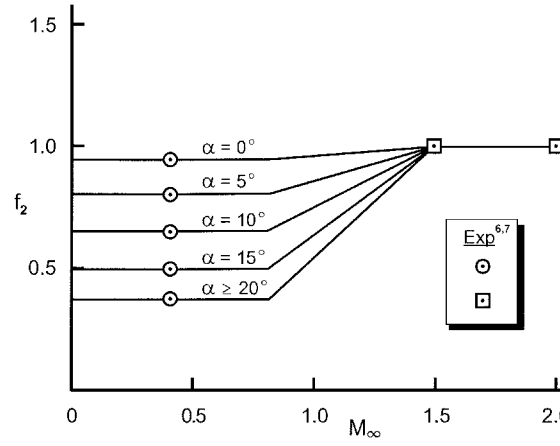

Fig. 7b Factor that corrects for use of secant vs tangent in normal force curve slope (δ_f = 10 deg).

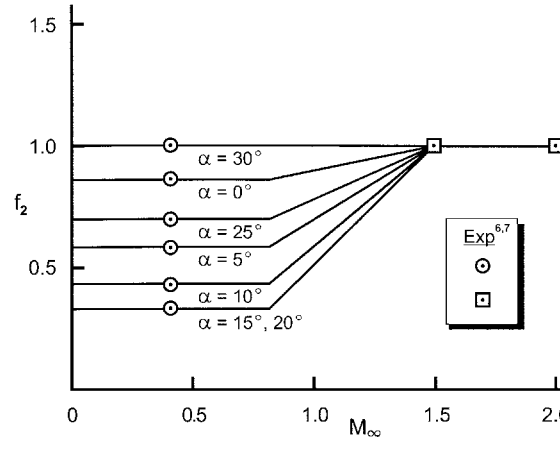

Fig. 7c Factor that corrects for use of secant vs tangent in normal force curve slope (δ_f = 30 deg).

Third, for a given wing size, $(C_{N_\alpha})_W$ is computed from the wing-alone solution in the AP02 at a given M_∞, α, AR, and λ. This value of $(C_{N_\alpha})_W$ must again be referenced to A_{ref}. Fourth, values of $k_{W(B)}$ and $k_{B(W)}$ are computed at a given α using the nonlinear control methodology in the AP02. This methodology uses slender-body theory as a basis for low AOA estimates and wind-tunnel data at high AOA to modify these estimates. Fifth, for a given value of δ_f, an effective value of δ_W can now be computed based on Eq. (7). This value of δ_W is the amount the entire wing is deflected to approximate the additional normal force of a wing due to a trailing-edge flap deflection of an amount δ_f.

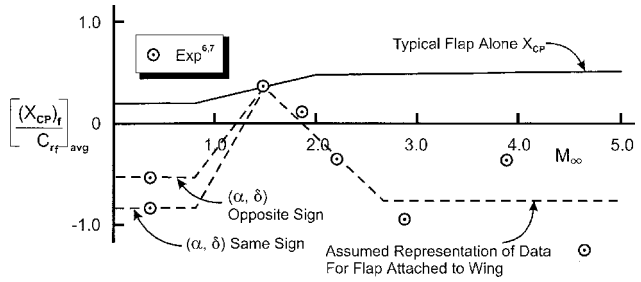

Fig. 8 Flap alone and trailing-edge flap attached to wing average c.p. over angle of attack range of 0–30 deg for various Mach numbers.

Equation (7) defines the equivalent fin deflection to give the same normal force that deflecting the rear part of the fin by an amount δ_f would give. The normal force coefficient of the flap or fin is computed from Eq. (6). That is,

$$(\Delta C_N)_f = f_1\left(C_{N_\alpha}\right)_f \delta_f \tag{8}$$

The question that we must now address is the pitching moment for the flap. When the entire wing is deflected by an amount δ_W defined by Eq. (7), the pitching moment for the wing will be based on the c.p. of the entire wing and not that due to the flap. Thus, to obtain the correct pitching moment for the flap, where the entire wing is deflected, a change in the c.p. must be calculated.

Most trailing-edge flaps under consideration have a fairly high aspect ratio with a fairly small root chord. The initial thought by the authors was to assume that the c.p. of the normal force generated by the trailing-edge flap would be similar to that on a high aspect ratio wing alone. That is, for subsonic flow, the c.p. would be around the quarter-chord location and then transition to the half-chord location at around $M_\infty = 2.0$. However, when this assumed location was compared to the experimental data of Refs. 6 and 7, it was clear that this assumption of c.p. location was not correct. It is believed that the reason the c.p. assumption was not correct is that the flap cannot be treated as a wing in isolation at most Mach numbers. At a Mach number of 1.5, the assumption of quarter-chord transitioning to half-chord was a good assumption supersonically (Fig. 8). However, at other Mach numbers, assuming that the c.p. of the flap normal force could be treated similar to a high aspect ratio wing in isolation became increasingly erroneous, as can be seen by the experimental data of Fig. 8. On review, the authors believe that the physics of the flow can explain the Fig. 8 experimental data. That is, as Mach number increases and the trailing-edge flap is deflected, a shock is created ahead of the leading edge of the flap. This shock, in turn, creates a high-pressure region on the wing where the flap is attached. This high-pressure region is the reason for the experimental c.p. of the flap normal force actually lying ahead of the leading edge of the flap (Fig. 8). The dashed line in Fig. 8 is the new assumed c.p. of the flap normal force as a function of Mach number. Notice that, in Fig. 8, $[(X_{CP})_f/C_r]_{av}$ represents the average c.p. over the AOA range from 0 to 30 deg as a fraction of the root chord of the flap.

At a subsonic Mach number of 0.4, the c.p. also lies ahead of the flap. If the flap deflection has the same sign as the AOA, this c.p. location is about 0.7 flap chord lengths ahead of the flap leading edge. If the flap deflection is of opposite sign than the AOA, the c.p. is about 0.4 flap chord lengths ahead of the flap leading edge. For Mach numbers from 0 to 0.8, it is assumed that these values of 0.4 and 0.7 chord lengths hold constant. For Mach numbers from 0.8 to 1.5, it is assumed that the location of the flap c.p. varies linearly between the values at $M_\infty = 0.8$ and 1.5.

The physics that cause the c.p. to move ahead of the flap are believed to be different for the subsonic and supersonic cases. Supersonically, it is believed that viscous effects, as well as the shock structure, are the dominant features. However, subsonically, it is believed that the flap deflection rearranges the pressure distribution on the wing ahead of the flap, as well as the viscous effects, that are present at all Mach numbers. The rearrangement of the pressure distribution on the wing ahead of the flap occurs because, in subsonic flow, disturbances in the flow can feed forward, whereas supersonically they can only do so through the boundary layer.

From a practical standpoint, the effect of the flap c.p. shift diminishes its effectiveness somewhat in generating the trim AOA. The slight loss of effectiveness occurs because the c.p. of the normal force actually lies in front of the flap at most Mach numbers, decreasing the moment somewhat and, hence, decreasing the trim AOA. On the other hand, if the flap is located near the base of a fairly long body, a 1–4-in. shift in the c.p. forward can be fairly small in terms of the overall moment arm. The amount of normal force created does not seem to be affected by the forward shift in the c.p. for trailing-edge flaps.

The c.p. of the trailing-edge flap is, therefore,

$$(X_{CP})_f/\ell_{ref} = \left[(X_{LE})_W + C_{r_W} - C_{r_f} f_3 - X_{ref}\right]\Big/\ell_{ref} \tag{9}$$

The term f_3 of Eq. (9) is based on the empirically defined dotted lines of Fig. 8. That is,

$f_3 = +1.5$

for $M_\infty \le 0.8$ and (α, δ) opposite signs

$= +1.8$ for $M_\infty \le 0.8$ and (α, δ) same signs

$f_3 = 2.53 - 1.29M_\infty$

for $0.8 < M_\infty \le 1.5$ and (α, δ) opposite signs

$= 3.17 - 1.71M_\infty$

for $0.8 < M_\infty \le 1.5$ and (α, δ) same signs

$f_3 = -0.84 + 0.96M_\infty$

for $1.5 < M_\infty \le 2.7$, same or opposite sign

$= 1.75$ for $M_\infty > 2.7$, same or opposite sign (10)

By the use of Eqs. (9) and (10), the change in pitching moment created by the wing being deflected to simulate the trailing-edge flap deflection is then

$$(\Delta C_M)_f = -[(\Delta C_N)_f/\ell_{ref}]\{[(X_{CP})_f - (X_{CP})_W] + [(X_{CP})_W - X_{CG}]\} \tag{11}$$

Equation (11) represents the pitching moment coefficient of any configuration where the trailing-edge flap deflection is approximated by deflecting the full wing. The first term of Eq. (11) represents the difference in the c.p. between the flap and wing, whereas the second term represents the c.p. of the wing normal force term relative to a reference location, which is here taken to be the c.g. of the vehicle. Of course, the c.p. of the wing is computed in the AP02 using linear theory methods at low AOA and transitions to the centroid of the wing planform area at high AOA.

The major focus in the analysis for estimating the aerodynamics of trailing-edge flaps has been to determine an equivalent tail deflection that will give normal force and pitching moments equal to those when the flap is deflected. No mention of axial force has been made to this point. The axial force coefficient will be different for an equivalent wing deflection based on a flap deflection δ_f. The flap deflection will generate an additional axial force term because δ_f will be generally much larger than δ_W. An approximate relation that can be used to calculate the increment in axial force coefficient that results from estimating the aerodynamics based on a wing deflection of δ_W vs a flap deflection of δ_f is

$$(\Delta C_A)_f \cong (\Delta C_N)_f[\sin|\delta_f| - \sin|\delta_W|] \tag{12}$$

$(\Delta C_N)_f$ of Eq. (12) is the additional normal force contribution due to the flap. Here $\sin|\delta_f|$ takes the component of this normal force term in the axial direction, and $\sin|\delta_W|$ subtracts off of the component of axial force of the wing because this is automatically included in the AP02 calculations. Leaving this term in the calculations would cause us to account for the wing deflection axial force contribution twice.

Results and Discussion

Equations (8) and (11) define the theoretical change in normal force and pitching moment coefficients due to a flap deflection. The value of $(\Delta C_N)_f$ computed by the theory is that value defined by

$$(\Delta C_N)_f = (C_N)_{\delta_W=0} - (C_N)_{\delta_W\neq 0} \tag{13a}$$

The value of δ_W in Eq. (13a) is obtained from Eq. (7) using the process defined earlier in the analysis section of this report. By the use of the values of δ_W from Eq. (7) in the AP98, values of $(C_N)_{\delta_W=0}$ and $(C_N)_{\delta_W\neq 0}$ of Eq. (13a) can be computed, and then $(\Delta C_N)_f$ can be defined theoretically. This value of $(\Delta C_N)_f$ can then be compared to experimental data where $(\Delta C_N)_f$ is obtained using experimental data for $(C_N)_{\delta_f=0}$ and $(C_N)_{\delta_f\neq 0}$. That is,

$$(\Delta C_N)_f = (C_N)_{\delta_f=0} - (C_N)_{\delta_f\neq 0} \tag{13b}$$

Likewise, experimentally measured values of $(\Delta C_M)_f$ can be defined as

$$(\Delta C_M)_f = (C_M)_{\delta_f=0} - (C_M)_{\delta_f\neq 0} \tag{14}$$

and compared to theoretical values computed from Eq. (11). $(\Delta C_N)_f$ of Eq. (11) comes from the theoretical values defined by Eq. (13a). Thus, comparison of $(\Delta C_N)_f$ values obtained by Eq. (13a) to those of Eq. (12) and comparison of $(\Delta C_M)_f$ values obtained from Eq. (11) to those of Eq. (14) will allow us to determine the validity and accuracy of the new theory.

The first set of data that we will consider is from Ref. 6. The configuration tested in the wind tunnel is shown in Fig. 3. Figures 9–11 compare theory and experiment for $(\Delta C_N)_f$ and $(\Delta C_M)_f$ at $\delta_f = -20$ deg and Mach numbers 1.5, 2.96, and 4.63. Similar results for other Mach number cases can be found in Ref. 2. Results are plotted as a function of AOA up to 30 deg. For Mach number 1.5, experimental data were not available up to 30-deg AOA, and so data were shown where available. As seen in Figs. 9–11, the theory does a reasonable job in matching the data for both $(\Delta C_N)_f$ and $(\Delta C_M)_f$, except at $M_\infty = 4.63$ and $\alpha \geq 20$ deg. At these conditions, the theory overpredicts the normal force and pitching moment increments somewhat. However, because this region is beyond the anticipated practical range of usage ($M_\infty < 2.0$, $\alpha < 20$, and $|\delta_f| < 30$ deg), no effort will be made to try to improve on the theory at this condition.

Also shown in the $(\Delta C_M)_f$ portion of Figs. 9–11 are the results of assuming that the c.p. of the flap is based on the flap in freestream flow and with the flap attached to the trailing edge. The flap attached

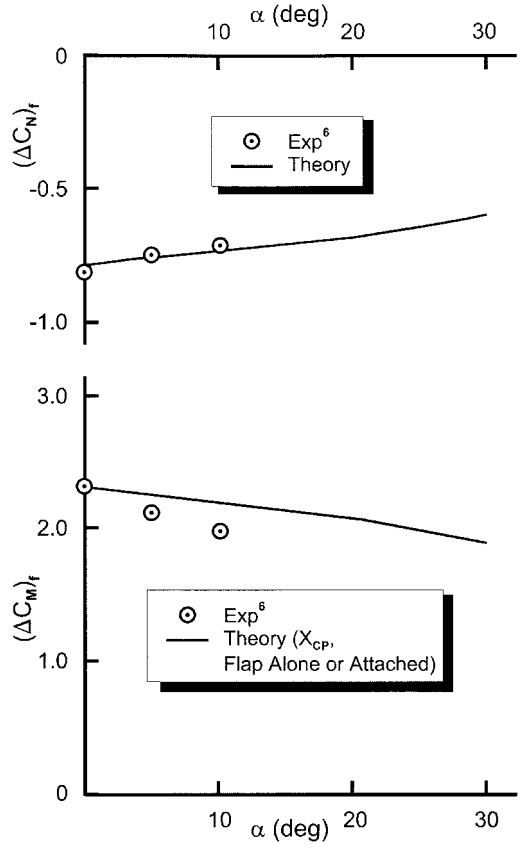

Fig. 9 Comparison of theory and experiment for normal force and pitching moment coefficients of trailing-edge flaps ($M_\infty = 1.5$ and $\delta_f = -20$ deg).

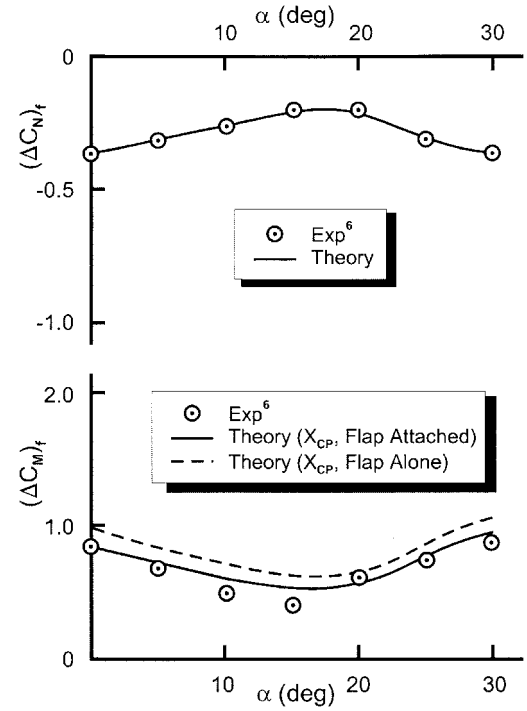

Fig. 10 Comparison of theory and experiment for normal force and pitching moment coefficients of trailing-edge flaps ($M_\infty = 2.96$ and $\delta_f = -20$ deg).

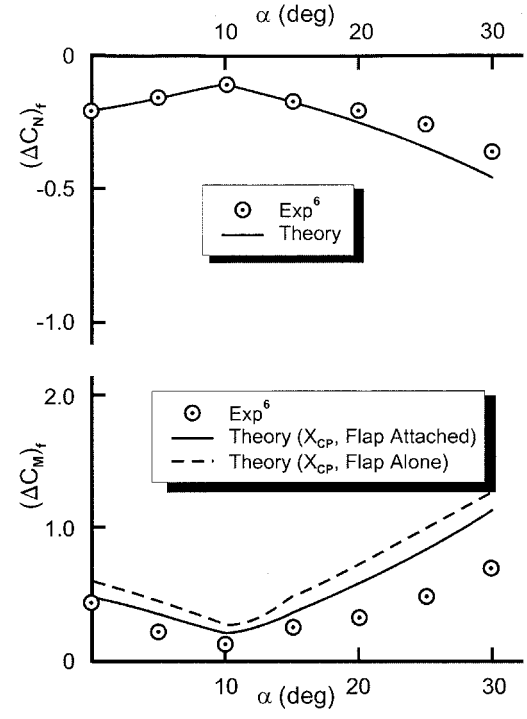

Fig. 11 Comparison of theory and experiment for normal force and pitching moment coefficients of trailing-edge flaps ($M_\infty = 4.63$ and $\delta_f = -20$ deg).

to the trailing-edge computations takes into account the c.p. shift shown in Fig. 8. Note that at $M_\infty = 1.5$ no shift is shown, and so the Fig. 9 pitching moment results show no change between the flap alone and the flap attached. However, Figs. 10 and 11 show a change in pitching moment between flap alone and the flap attached. As seen in Figs. 10 and 11, use of Fig. 8 results tends to improve pitching moment calculations over assuming the flap alone.

Also note that all of the theoretical calculations shown in Figs. 9–11 were computed by using the AP02 in conjunction with Eq. (7), as described in the "Analysis" section of the paper.

Figures 12 and 13 compare theory and experiment for $(\Delta C_N)_f$ and $(\Delta C_M)_f$ as a function of flap deflection at 10-deg AOA and

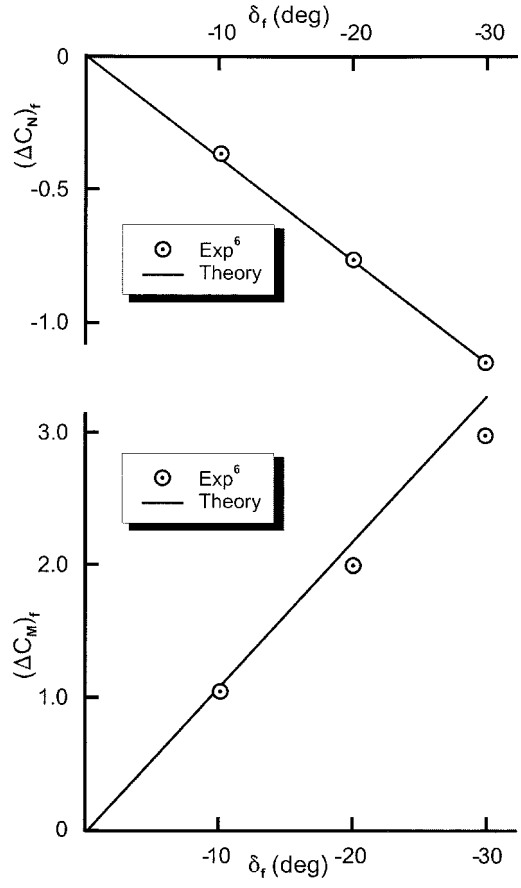

Fig. 12 Comparison of theory and experiment for normal force and pitching moment coefficients of trailing-edge flaps ($M_\infty = 1.5$ and $\alpha = 10$ deg).

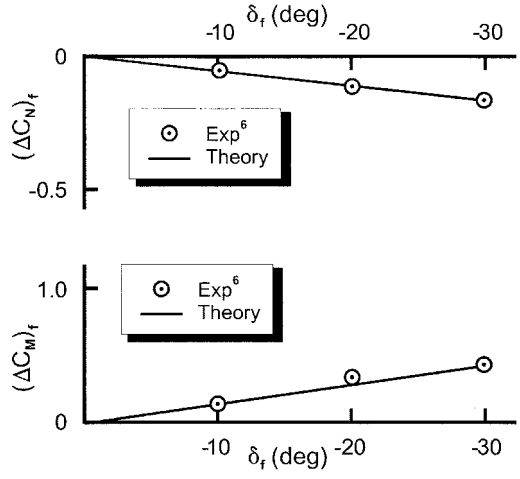

Fig. 13 Comparison of theory and experiment for normal force and pitching moment coefficients of trailing-edge flaps ($M_\infty = 4.63$ and $\alpha = 10$ deg).

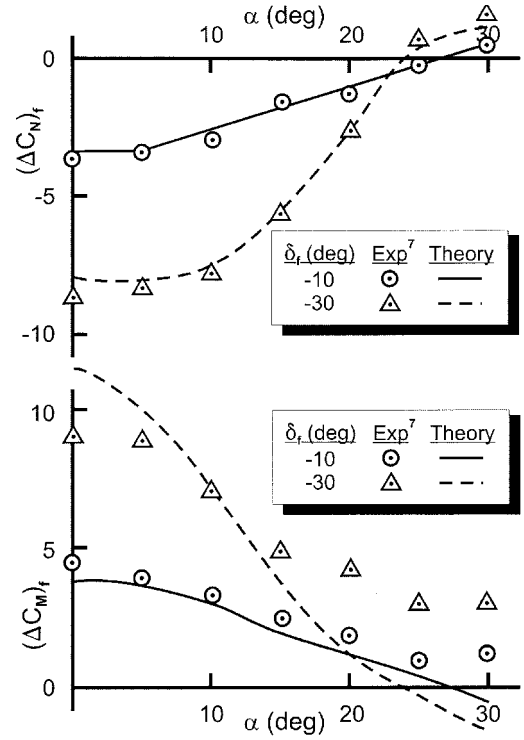

Fig. 14 Comparison of theory and experiment for normal force and pitching moment coefficients of trailing-edge flaps ($M_\infty = 0.4$ and δ_f negative).

for two of the Mach numbers of the Ref. 6 database. Again, similar results for other Mach number cases can be found in Ref. 2. Figures 12 and 13 are believed to be a more realistic representation of the practical case, where trim is expected to occur for $\alpha \leq 10$ deg with the flap deflected as high as -30 deg. As seen in Figs. 12 and 13, the theory and experiment are in fairly good agreement. All pitching moment data in Figs. 12 and 13 assume the Fig. 8 c.p. shift. Note also that the theory shows a linear variation of $(\Delta C_N)_f$ and $(\Delta C_M)_f$ for $M_\infty \geq 1.5$ and δ_f to -30 deg for the small AOA of 10 deg.

Reference 7 represents the only subsonic database the authors found in the literature. The configuration tested is shown in Fig. 4. The ogive of the Fig. 4 configuration can be elliptical or a circular cylinder tangent ogive. The case on which the change in pitching moments and normal force coefficients was determined was based on an elliptical nose. However, because the data used were $(\Delta C_N)_f$ and $(\Delta C_M)_f$, it is expected that the body shape will have little impact because the same body shape is used for the $\delta_f = 0$ case and the $\delta_f \neq 0$ case. Reference 7 has both positive and negative values of δ_f available. Unfortunately, $M_\infty = 0.4$ was the highest freestream Mach number considered, and AOA to 30 deg were also included in the test series.

Figure 14 compares the theory and experiment for $(\Delta C_N)_f$ and $(\Delta C_M)_f$, where δ_f is negative for α up to 30 deg. Note that excellent agreement for $(\Delta C_N)_f$ is obtained between theory and experiment for both $\delta_f = -10$ and -30 deg cases. Good agreement between theory and experiment is obtained for $(\Delta C_M)_f$ for the $\delta_f = -10$ deg case up to α of about 20–25 deg, where the theory and experiment start to depart. For $\delta_f = -30$ deg, comparison of theory and experiment for $(\Delta C_M)_f$ is quite acceptable for α up to 20 deg. The trim AOA occurs at about 6 deg for $\delta_f = -10$ deg and at about 14.8 deg for $\delta_f = -30$ deg. In other words, good accuracy in both $(\Delta C_N)_f$ and $(\Delta C_M)_f$ can be obtained up to and slightly beyond the trim AOA, which is most critical. For α above the trim value, accuracy of $(\Delta C_N)_f$ and $(\Delta C_M)_f$ is not as important, and, thus, no attempt was made to try to improve the theory for these conditions.

Figure 15 gives the complimentary results to the Fig. 14 case, except that here δ_f is positive. Whereas trim cannot occur because α and δ_f are of the same sign, and the configuration is tail controlled, it is still of interest to see how well the theory compares to data for

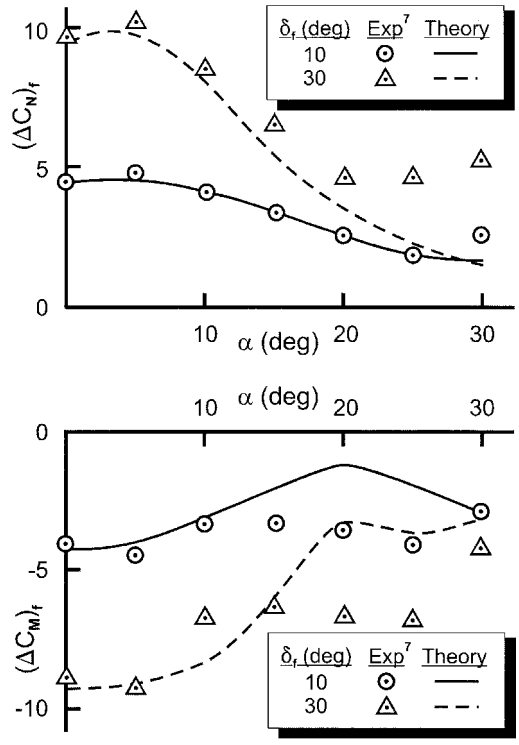

Fig. 15 Comparison of theory and experiment for normal force and pitching moment coefficients of trailing-edge flaps (M_∞ = 0.4 and δ_f positive).

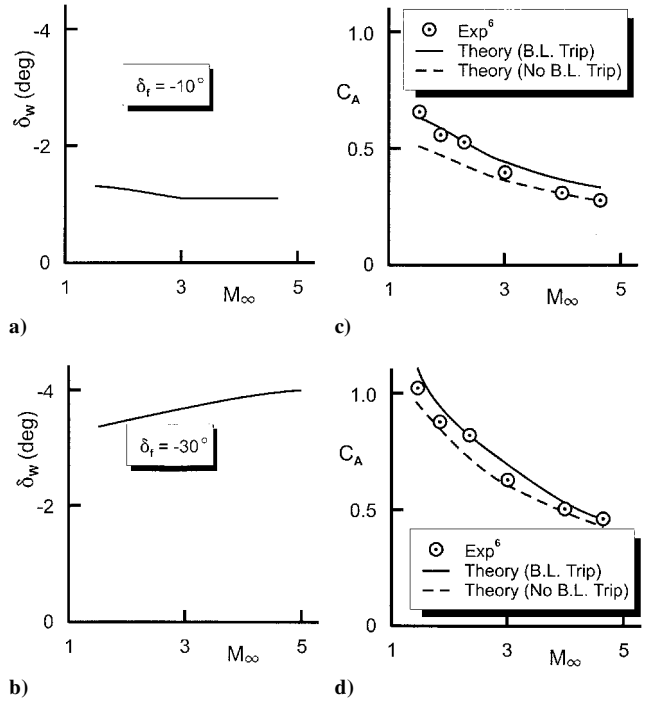

Fig. 16 Comparison of theory and experiment for axial force coefficient at various values of flap deflection and as represented by an equivalent deflection of entire wing at α = 0 deg (R_N/ft = 2.5 × 10^6).

conditions where trim is not possible. As seen in Fig. 15, agreement between theory and experiment for both $(\Delta C_N)_f$ and $(\Delta C_M)_f$ is quite good up to an α of about 15 deg. Above α of 15 deg, both $(\Delta C_M)_f$ and $(\Delta C_N)_f$ deviate from the experiment at most conditions. Again, because this is not a practical set of conditions for trim, no effort has been made to improve $(\Delta C_N)_f$ and $(\Delta C_M)_f$ for α above 15 deg, and δ_f is positive.

Figure 16 compares the theory and experiment for an axial force coefficient where the trailing-edge flap has been deflected −10 and −30 deg, respectively. The equivalent value of δ_W corresponding to $\delta_f = -10$ and −30 deg, respectively, is shown in Figs. 16a and 16b as a function of freestream Mach number. Note that δ_W is only a small fraction of δ_f. The wing area is 8.67 times that of the trailing-edge flap. In Figs. 16c and 16d are the axial force coefficient based on the AP02 calculations plus the value defined by Eq. (12). Two cases are shown for the theory: one where the wind-tunnel model has a boundary-layer trip and one where no boundary-layer trip is present. The Reynolds number for the tests was 2.5 × 10^6. According to Ref. 6, a boundary-layer trip was present. Based on comparison of theory and experiment, it appears that the boundary-layer trip was effective in producing a turbulent boundary layer over the surface at the lower supersonic Mach numbers. However, at the higher supersonic Mach numbers, it is speculated that the flow partially transitions back to laminar over much of the body and large wing for the $\delta = -10$ deg case. This relaminarization of the flow is speculated to be the reason that the theory with no boundary-layer trip option agrees closer to the wind-tunnel data at high supersonic Mach number than does the theory that assumes turbulent flow over the entire surface of the model at all Mach numbers. If the preceding hypothesis of relaminarization of the flow is correct, the theory predicts the experimental data quite nicely. If this hypothesis is not correct, then the theory is high for Mach numbers of 3.0 and greater.

The Ref. 7 database also contained axial force data. Unfortunately, the base drag term was subtracted out, only one fin was deflected, and the numbers for no fin deflection were small and irregular. As a result, it was believed that an accurate value of experimental data for the axial force would be difficult to obtain, and, therefore, no comparisons of axial force coefficient are shown at subsonic Mach numbers.

Conclusions

An improved semiempirical method has been developed to estimate the static aerodynamics generated by a trailing-edge flap. The method is based on deflecting the full wing or tail surface by an amount that allows the normal force coefficient to be equal to that generated by the flap deflected. A transfer in pitching moments is derived to account for the difference in pitching moment when a full wing vs a trailing-edge flap is deflected. Also, an approximate relationship is given that accounts for the additional axial force coefficient that is not accounted for based on a full wing deflected by a small amount vs a trailing-edge flap deflected by a larger amount.

When the new semiempirical method and experimental data were compared, the following observations were made:

1) Normal force coefficient predictions at supersonic speeds were very good, except at the highest Mach numbers ($M_\infty = 4.63$) and AOA ($\alpha > 25$ deg), where the predictions were only fair.

2) Pitching moment coefficient predictions at supersonic speeds were fair to good at all conditions considered ($1.5 \le M_\infty \le 4.63$, $0 \le \alpha \le 30$, and $-30 \le \delta_f \le 0$). The worst case agreement was, again, for $M_\infty = 4.63$ and $\alpha > 20$ deg.

3) Axial force coefficient predictions for supersonic conditions were found to be reasonable. However, the accuracy was seen to be dependent on whether the boundary layer on the wind-tunnel model remained turbulent at $M_\infty \ge 2.3$ vs returning to laminar flow over the model.

4) At subsonic flow, the only data available to the authors were at $M_\infty = 0.4$. For this Mach number, it was found the predictions for both normal force and pitching moment coefficients were acceptable up to and slightly past the trim AOA. For larger flap deflections, the accuracy of the predictions was acceptable at AOA that exceeded trim conditions by about 5 deg. However, because trim and slightly past trim are of the most practical interest, this problem was not seen as a major limitation.

A linear interpolation of the empirical factors used in the derivation process was assumed between Mach numbers of 0.8 and 1.5. Also, values of these factors were assumed to be constant below $M_\infty = 0.4$ and above $M_\infty = 4.63$, where no data were available.

Additional wind-tunnel data are needed to refine and validate the new semiempirical model. Specifically, data are needed when the AOA and flap deflection are of the same sign at supersonic speeds. Data are needed for Mach numbers between 0.4 and 1.5 as

well. However, until additional data become available, the model derived here uses engineering judgment to fill in these gaps and allows the model to be operational over the practical AOA, Mach number, and control deflection range for which trailing-edge flaps are contemplated for use.

References

[1]Moore, F. G., McInville, R. M., and Hymer, T. C., "The 1998 Version of the NSWC Aeroprediction Code: Part I—Summary of New Theoretical Methodology," U.S. Naval Surface Warfare Center, Dahlgren Div., NSWCDD/TR-98/1, Dahlgren, VA, April 1998.

[2]Moore, F. G., and Hymer, T. C., "A Semiempirical Method for Predicting Aerodynamics of Trailing Edge Flaps," U.S. Naval Surface Warfare Center, Dahlgren Div., NSWCDD/TR-01/30, Dahlgren, VA, June 2001.

[3]Blake, W. B., and Burns, K. A., "Missile Datcom: Recent Enhancements Including Trailing Edge Flap Effects," AIAA Paper 94-0027, Jan. 1994.

[4]Hoak, D. E., "USAF Stability and Control DATCOM," U.S. Air Force Wright Aeronautics Lab., AFWAL TR 83-3048, Wright–Patterson AFB, OH, Oct. 1960, rev. 1978.

[5]Goin, K. L., "Equations and Charts for the Rapid Estimation of Hinge-Moment and Effectiveness Parameters for Trailing-Edge Controls Having Leading and Trailing Edges Swept Ahead of the Mach Lines," NACA TR 1041, 1951.

[6]Triscott, C. D., Jr., "Longitudinal Aerodynamic Characteristics at Mach 1.50 to 4.63 of a Missile Model Employing Various Canards and a Trailing-Edge Flap Control," NASA TM X-2367, Oct. 1971.

[7]Baldwin, A. W., and Adamczak, D. W., "Experimental Evaluation of Aerodynamic Control Devices for Control of Tailless Fighter Aircraft," U.S. Air Force Research Lab., Flight Dynamics Directorate, WL-TM-92-318, Wright–Patterson AFB, OH, April 1992.

M. S. Miller
Associate Editor